

## Diamond-carbide-silicon composite „skeleton“ as a promising material for X-ray optical substrates

© M.V. Zorina,<sup>1</sup> M.S. Mikhailenko,<sup>1</sup> A.E. Pestov,<sup>1</sup> M.N. Toropov,<sup>1</sup> A.K. Chernyshev,<sup>1</sup> N.I. Chkhalo,<sup>1</sup> S.K. Gordeev,<sup>2</sup> V.V. Vitkin<sup>3</sup>

<sup>1</sup> Institute of Physics of Microstructures, Russian Academy of Sciences, 603087 Nizhny Novgorod, Russia

<sup>2</sup> CSRI of materials, 191014 St Petersburg, Russia

<sup>3</sup> ITMO University, 197101 St Petersburg, Russia  
e-mail: aepestov@ipm.sci-nnov.ru

Received April 6, 2022

Revised April 6, 2022

Accepted April 6, 2022

The paper proposes the use of diamond-carbide-silicon composite „Skeleton“<sup>®</sup> coated with amorphous silicon as substrates for multilayer X-ray mirrors for powerful synchrotron radiation sources (3+ and 4th generation). The surfaces with the following parameters were obtained using standard deep polishing methods: flatness at the level of  $RMS_{90\%} = 54.2$  nm; effective roughness  $\sigma_{\text{eff}} \sim 1.0$  nm; high-frequency roughness  $\sigma_{2 \times 2} \sim 0.1$  nm.

**Keywords:** x-ray optics, x-ray mirrors, substrates for x-ray mirrors, roughness.

DOI: 10.21883/TP.2022.08.54572.85-22

### Introduction

With the development of powerful synchrotron radiation sources (3+ and 4th generation), as well as free electron lasers [1–3], the problem of precision X-ray optical elements resistant to large (up to several kW) radiation and thermal loads has become acute. Currently, it is believed that single-crystal silicon can be considered primarily as a substrate material for mirrors operating under such powerful radiation beams [4–6]. Other materials, including silicon carbide and metals (copper, aluminum, beryllium), are significantly inferior to it in terms of their thermal and physical characteristics [7,8]. Monocrystalline diamond has the best characteristics for these properties, however, due to the complexity of obtaining this material with dimensions of tens of centimeters, it is mainly used as crystal monochromators, X-ray beam splitters and refractive lenses [9–11], but not as substrates for multilayer X-ray mirrors.

As for the surface roughness of monocrystalline silicon, there is currently a proven polishing technique that provides a surface roughness at the level of 0.1 nm [12], but significant difficulties arise with shaping. Silicon, as a rule, is processed on an ultra-precision micro milling machine with a diamond cutter [13–15]. This technology is quite well developed, but has a number of disadvantages. First of all, it is the forming near-surface disturbed layer and increased roughness, in particular, furrows are formed with a cutter pitch [13,14]. These defects are removed by chemical-dynamic etching, however, with this method of processing, the surface shape parameters often degrade.

As an alternative to crystalline materials, primarily monocrystalline silicon, a diamond-carbide-silicon (DCS) composite „Skeleton“<sup>®</sup> [16] can be considered. The DCS structure „Skeleton“<sup>®</sup> is formed by diamond grains bound into a single composite by a silicon carbide matrix. The material is inferior in its physico-mechanical and thermophysical properties only to monocrystalline diamond, however, it allows forming a workpiece of almost arbitrary sizes and shapes („net-shape“-technology, due to the implementation of chemical reactions in the volume of the workpiece). Thus, the production technology makes it possible to produce, among other things, a developed back side of the substrate to increase heat transfer during liquid cooling. The use of this material as substrates for X-ray optical elements operating under powerful synchrotron radiation beams can make it possible to switch from monocrystalline materials that are difficult to process to the traditional technology of finishing shaping and polishing used on amorphous blanks, such as fused quartz, Zerodur, sital, etc. This approach combines mechanical lapping and grinding-polishing, as well as finishing ion-beam correction of local shape errors.

As part of this study, the certification of surfaces obtained during machining was carried out and the prospects for the use of substrates based on DCS „Skeleton“<sup>®</sup> as substrates for X-ray optical applications were evaluated.

### 1. Measurement procedure

The surface roughness was certified using the atomic force microscope (AFM) Ntegra Prima (NT-MDT). The photographic image of the stand is presented in Fig. 1.

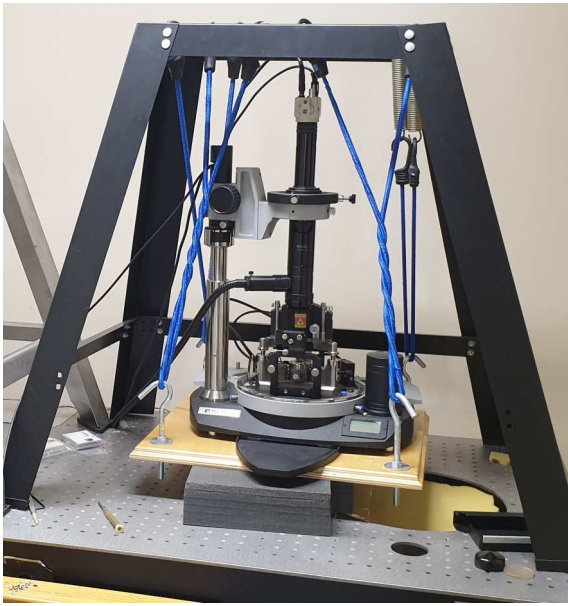


Figure 1. ACM Ntegra Prima (NT-MDT).

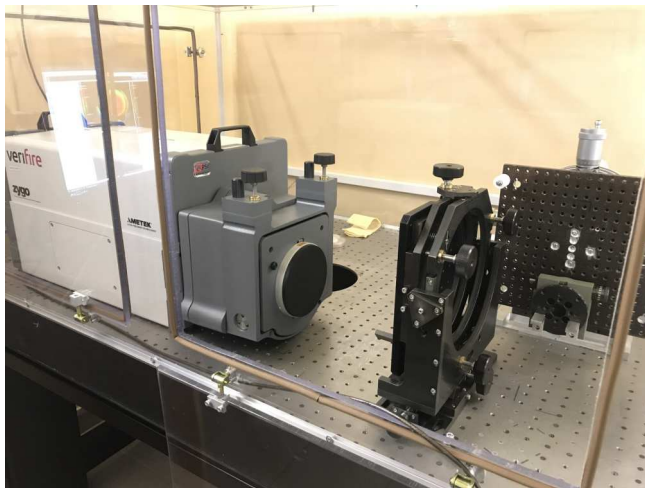


Figure 2. Laser Interferometer ZYGO Verifier 4.

Frames from  $2 \times 2$  were measured to  $40 \times 40 \mu\text{m}$ . Based on the measurement results, the PSD function (Power Spectral Density) of the roughness was restored and the effective roughness was determined by it. The PSD function — the power spectral density function is determined by the formula (1), and in fact is a roughness decomposition over the frequencies of the spatial spectrum [17]:

$$\text{PSD}(\nu) = |\hat{F}[z(\vec{\rho})]|, \quad (1)$$

where  $z(\vec{\rho})$  — the height of the surface at the point specified by the radius vector ( $\vec{\rho}$ );  $\hat{F}$  — Fourier transform. If  $L$  is the linear size of the scanning area (AFM frame) and  $N$  is the number of points (pixels), then the module of the spatial frequency vector in which the PSD function is calculated lies in the range from  $\nu_{\min} = 1/L$  to  $\nu_{\max} = N/2L$ .

To switch to the language of roughness, the concept of effective roughness (2) is used, which is an integral of the PSD function in a certain range of spatial frequencies:

$$\sigma_{\text{eff}}^2 = \int_{\nu_{\min}}^{\nu_{\max}} \text{PSD}(\nu) d\nu. \quad (2)$$

In our case, the spatial frequency interval was  $\nu \in [2.5 \cdot 10^{-2} - 6.4 \cdot 10^1 \mu\text{m}^{-1}]$ . This range covers the entire spectrum of roughness with lateral dimensions from  $40 \mu\text{m}$  to  $15 \text{nm}$ , which affect both the imaging properties of the optical element and the reflective characteristics of multilayer X-ray mirrors.

Surface flatness measurements were investigated using a ZYGO Verifire 4 laser interferometer (ZYGO Corporation). The photo of the interferometer is shown in Fig. 2.

According to the measurement data, the surface parameters were calculated: PV (Peak-to-Valley — span of heights on the surface) and RMS (standard deviation of the surface from the plane).

## 2. Measurement results

As experimental samples, 4 plates with a diameter of  $40 \text{mm}$  were proposed for the study, the composition of DCS „Skeleton“®: diamond — 60 vol.%, SiC — 34 vol.%, Si — 6 vol.%. The high hardness and wear resistance of the composite extremely complicate its mechanical processing, including grinding and polishing. To solve this problem, a thin (about  $0.5 \text{mm}$ ) coating of amorphous silicon was formed on substrates made of DCS „Skeleton“®. This coating lends itself well to polishing and, due to its small thickness, should not reduce the thermal characteristics of the substrate. Thus, the total thickness of the sample was  $4.5 \text{mm}$ . All samples showed similar parameters, both in terms of surface roughness and flatness. Fig. 3 shows typical AFM surface frames (sample SK2).

Fig. 4 shows the curve of the PSD function of the surface roughness of the sample SK2, constructed according to AFM measurements.

As you can see, there is a gap in the curves of PSD functions constructed from frames of different sizes, which is explained by a sharp increase in the roughness value when scratches hit the frame with an increase in its size. The integral value of the effective surface roughness was  $\sigma_{\text{eff}} = 0.8 \text{nm}$  over the entire range of spatial frequencies  $\nu \in [2.5 \cdot 10^{-2} - 6.3 \cdot 10^1 \mu\text{m}^{-1}]$ . The main contribution to the roughness value is the presence of a large number of deep (depth  $\sim 10 \text{nm}$ ) scratches, the areas between the scratches (frames  $2 \times 2 \mu\text{m}$ ) show good surface smoothness ( $\sigma_{2 \times 2} \sim 0.1 \text{nm}$ ).

Fig. 5 shows the measurement screen from the ZYGO interferometer.

The maximum height span was more than  $0.75 \mu\text{m}$ , with a root-mean-square error of the surface shape of

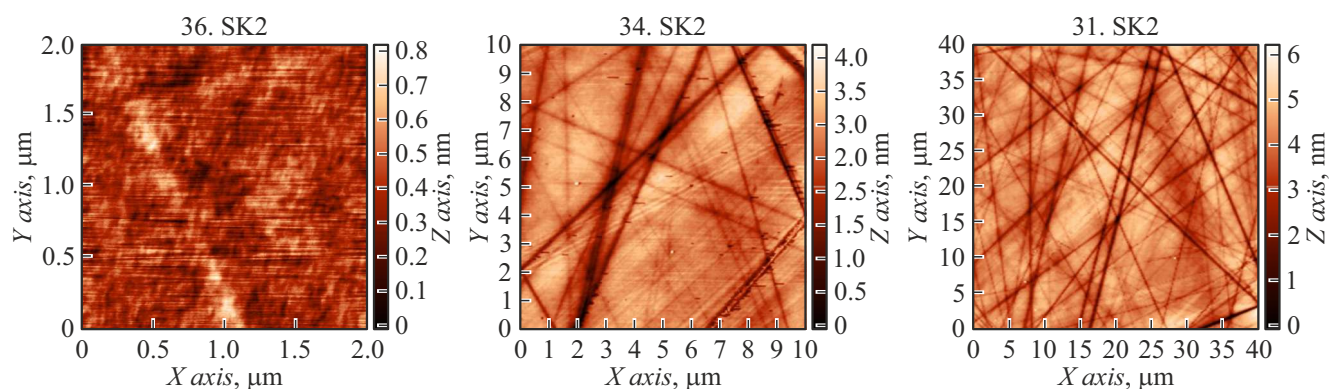


Figure 3. AFM SK2 sample surface frames: *a* — frame 2 × 2, *b* frame 10 × 10, *c* — frame 40 × 40 μm.

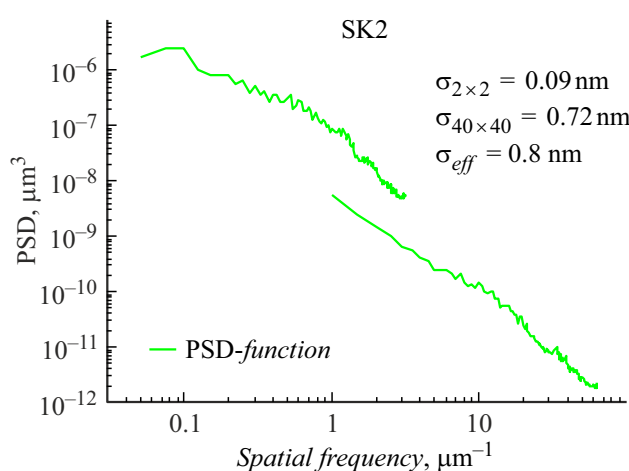


Figure 4. PSD-surface roughness functions of the SK2 sample, constructed from AFM data.  $\sigma_{eff} = 0.8$  nm.

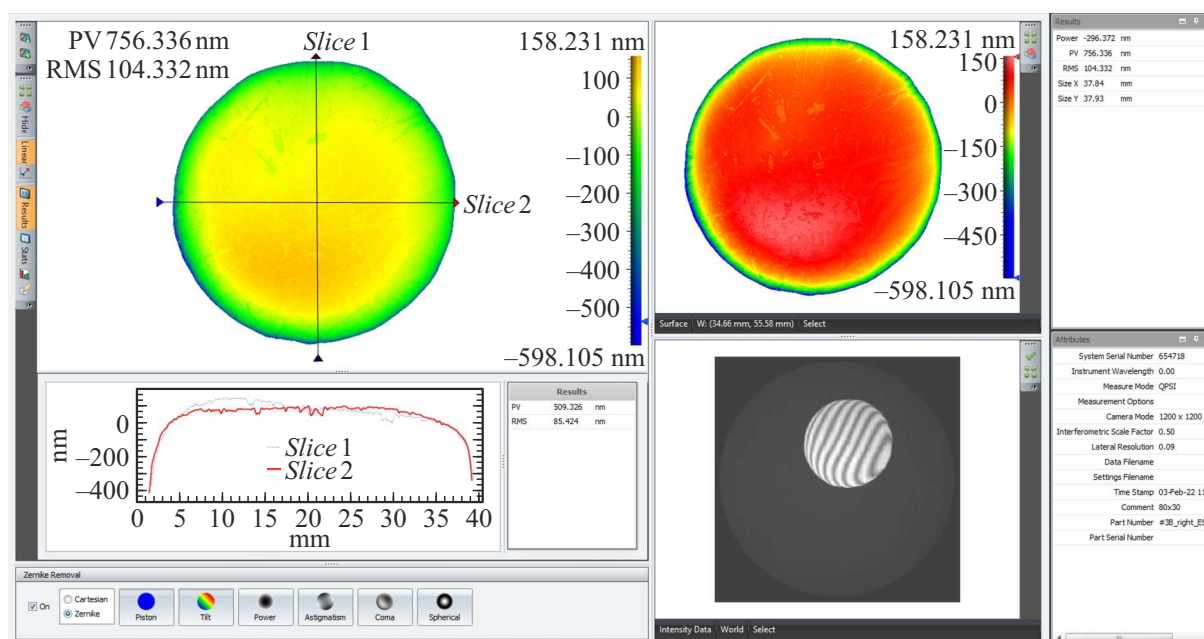
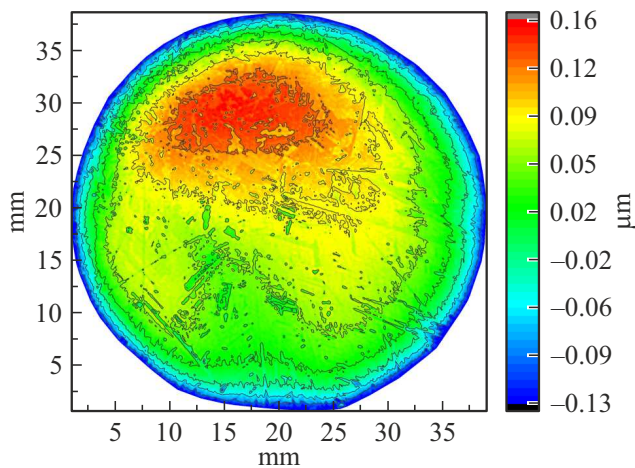


Figure 5. Results of measuring the shape of the surface of the SK3 sample. PV = 0.76 μm, RMS = 104.3 nm.



**Figure 6.** 90% of the sample surface SK3, PV90% = 287 nm, RMS90% = 60.1 nm.

more than 100 nm. The maximum „blockage“ in flatness is observed at the edges of the sample, while in the central region (90% of the surface level from the maximum) the surface characteristics are much better: PV90% = 287 nm, RMS90% = 60.1 nm, however, macroscopic defects (scratches, potholes) are manifested (Fig. 6).

The spread of parameters across all four samples was:  $\sigma_{\text{eff}} = 0.8\text{--}1.1$  nm, PV90% = 240–290 nm and RMS90% = 50–60 nm. Such a small spread of surface roughness and flatness parameters indicates a proven technology that allows to obtain surfaces with the parameters indicated above.

## Conclusion

The measurements carried out show high quality of high-frequency roughness ( $\sigma_{2 \times 2} \sim 0.1$  nm), which is at the level of values obtained on standard substrates for multilayer X-ray mirrors made of materials such as fused quartz, sitall, ULE, Zerodur. However, the average frequency roughness ( $\sigma_{40 \times 40}$ ) is at the level of 1.0 nm, which does not allow using surfaces prepared using this technology as substrates for multilayer X-ray mirrors. (The effective roughness in the entire range of spatial frequencies  $\nu \in [2.5 \cdot 10^{-2}\text{--}6.3 \cdot 10^1 \mu\text{m}^{-1}]$  should not be worse than 0.3 nm.) The main contribution to the value of the rms roughness of the mid-frequency range is made by numerous scratches with a width of about 100 nm and a depth of up to 10 nm.

The flatness of the surface is also noticeably inferior to the parameters obtained using traditional optical technologies (lapping allows you to obtain a surface with a height difference of PV < 100 nm and a standard deviation of the surface shape from the plane / sphere RMS < 10 nm). Nevertheless, the roughness values at the level of 1 nm allow us to hope that the use of lapping methods with finishing superpolishing developed in the work of [18], and precision

correction of shape errors, including ion-beam methods [19], will allow to obtain roughness and flatness at an acceptable level for X-ray optical applications.

## Funding

The study was carried out with the financial support of the Ministry of Science and Higher Education of the Russian Federation (agreement № 075-15-2021-1362).

## Conflict of interest

The authors declare that they have no conflict of interest.

## References

- [1] [Electronic resource] Available at: [http://www.esrf.eu/Apache\\_files/Upgrade/ESRF-orange-book.pdf](http://www.esrf.eu/Apache_files/Upgrade/ESRF-orange-book.pdf)
- [2] [Electronic resource] Available at: <https://www.maxiv.lu.se/about-us/>
- [3] S.V. Rashchenko, M.A. Skamarokha, G.N. Baranov, Ya.V. Zubavichus, I.V. Rakshun. AIP Conf. Proc., **2299**, 060001 (2020). DOI: 10.1063/5.0030346
- [4] A.R. Belurea, A.K. Biswas, D. Raghunathan, Rishipal, S. Bhartiya, R. Singh, S.K. Rai, R.S. Pawade, M.P. Kamath, N.S. Benerji. Mater. Today: Proceed., **26**, 2260 (2020). DOI: 10.1016/j.matpr.2020.02.490
- [5] L. Assoufid, H. Graafsma. MRS Bull., **42** (6), 418 (2017). DOI: 10.1557/mrs.2017.118
- [6] Z. Wang, L. Wu, Y. Fang, A. Dun, J. Zhao, X. Xu, X. Zhu. Micromachines, **13** (2), 318 (2022). DOI: 10.3390/mi13020318
- [7] P.Z. Takacs. Synchrotron Radiat. News., **2** (26), 24 (1989). DOI: 10.1080/08940888908261239
- [8] N.I. Chkhalo, M.V. Zorina, I.V. Malyshev, A.E. Pestov, V.N. Polkovnikov, N.N. Salashchenko, D.S. Kazakov, A.V. Miřkov, I.L. Strulya. Tech. Phys., **64** (11), 1596 (2019). DOI: 10.1134/S1063784219110070
- [9] D. Zhu, Y. Feng, S. Stoupin, S.A. Terentyev, H.T. Lemke, D.M. Fritz, M. Chollet, J.M. Glowina, R. Alonso-Mori, M. Sikorski, S. Song, T.B. van Driel, G.J. Williams, M. Messerschmidt, S. Boutet, V.D. Blank, Yu.V. Shvyd'ko, A. Robert. Rev. Sci. Instrum., **85** (6), 063106 (2014). DOI: 10.1063/1.4880724
- [10] K. Li, Y. Liu, M. Seaberg, M. Chollet, T.M. Weiss, A. Sakdinawat. Opt. Express., **28** (8), 10939 (2020).
- [11] M. Polikarpov, V. Polikarpov, I. Snigireva, A. Snigirev. Phys. Proced., **84**, 213 (2016). DOI: 10.1016/j.phpro.2016.11.037
- [12] [Electronic resource] Available at: <http://siliconwafers.net/>
- [13] N. Khatri, R. Sharma, V. Mishra, H. Garg, V. Karar. Adv. Mater. Proc., **2** (7), 425 (2017). DOI: 10.5185/amp.2017/704
- [14] L.N. Abdulkadir, K. Abou-El-Hosseini, A.I. Jumare, P.B. Odedyi, M.M. Liman, T.A. Olaniyan. Int. J. Adv. Manuf. Technol., **96**, 173 (2018). DOI: 10.1007/s00170-017-1529-x
- [15] A. Mir, X. Luo, K. Cheng, A. Cox. Int. J. Adv. Manuf. Technol., **94**, 2343 (2018). DOI: 10.1007/s00170-017-1021-7

- [16] C. Kataev, V. Sidorov, S. Gordeev. *Elektronika: NTB*, **3**, 60 (2011) (in Russian).
- [17] L. Peverini, E. Ziegler, T. Bigault, I. Kozhevnikov. *Phys. Rev. B*, **72**, 045445 (2005).
- [18] M.N. Toropov, A.A. Akhsakhalyan, M.V. Zorina, N.N. Salashchenko, N.I. Chkhalo, Yu.M. Tokunov. *Tech. Phys.*, **65** (11), 1873 (2020). DOI: 10.1134/S1063784220110262
- [19] I.G. Zabrodin, M.V. Zorina, I.A. Kas'kov, I.V. Malyshchev, M.S. Mikhailenko, A.E. Pestov, N.N. Salashchenko, A.K. Chernyshev, N.I. Chkhalo. *Tech. Phys.*, **65** (11), 1837 (2020). DOI: 10.1134/S1063784220110274